Determining constraints on the carbon budget during deglaciation with a new method of carbon isotope data analysis

Alice Nadeau*, Clarence Lehman†, Richard McGehee ‡, and Eville Gorham§

June 28, 2018

Keywords: Holocene; Paleoclimatology; Global; Data analysis; Carbon; Stable isotopes; Ice cores; Peatlands

Abstract

Recent data sets reveal the history of atmospheric carbon from the last glacial maximum (24kyBP) to the present — both total carbon and isotopic ratios. The question arises, what were the dynamical rates of transfer in and out of the atmosphere from the many possible sources and sinks, both biological and physical, and what known sources and sinks can be incorporated that put further constraints on the global carbon budget? Here we analyze the dynamics and incorporate one known large sink into the analysis — the ongoing growth of peatlands — revealing evidence for a large global source of biological carbon during deglaciation. We introduce a new analytical technique that will allow other sources and sinks to be incorporated, as they become known. Understanding the dynamics of carbon during the long-term changes occurring in glacial times can become part of the foundation for understanding the even larger changes occurring today.

1 Introduction

Recent understanding of the composition of carbon isotopes in the atmosphere has advanced our understanding of the progression of the carbon budget since the last glacial maximum [9, 26].

*Corresponding Author: nadea093@umn.edu; School of Mathematics, University of Minnesota
†Department of Ecology, Evolution, and Behavior, University of Minnesota
‡School of Mathematics University of Minnesota
§Department of Ecology, Evolution, and Behavior, University of Minnesota

Different physical, biological, and chemical processes favor one carbon isotope over the other, which can help identify possible carbon sources and sinks based on their isotopic signatures.

Isotopic signatures are commonly measured by δ^{13}C, measured permil (one-tenth of a percent, denoted ‰), normalized by a standard, and designed to accentuate small differences between samples (Supplementary Materials, Equation A1). The standard comes from fossilized *Belemnitella americana*, which has anomalously high carbon-13 content, in contrast with many direct biological pools. Most biological matter has a large negative δ^{13}C value because plants discriminate in favor of the lighter carbon-12 during photosynthesis. The δ^{13}C signature of plants ranges from about -11‰ to -33‰, depending on the type of photosynthesis employed by the plant [11]. Conversely, physical processes such as the formation of calcium carbonate or volcanic release tend to leave samples with a δ^{13}C signature closer to the standard (i.e. nearer 0‰). With this isotope information in mind, we have sought to understand the forces that affected the carbon budget during the Holocene.

Details of the carbon budget can be complex, varying with the kind of source or sink and with physical and temporal conditions. A growing biome, for example, will absorb carbon from the air during photosynthesis at one δ^{13}C ratio, respire carbon back into the air at a different ratio, and incorporate carbon into its tissues at a third ratio. When a component of the biome dies, decomposition will leave a fourth ratio of δ^{13}C in the biomass residue and will emit a fifth ratio into the atmosphere resulting from the decomposition (Figure 1).

Fortunately, for long-term effects on the atmosphere, it is only the net value of all these flows that is relevant. In the growth of a new forest following deglaciation, for example, carbon from the air will be incorporated into plant tissues above and below ground, with living total biomass saturating as the forest matures. However, carbon may continue to build up in residues for many millennia, as is the case for lake sediments and peatlands [13, 15, 18], and possibly northern forest soils. Rates of formation of cumulative residue must be accounted for as part of the long-term record, but not the individual transient fluxes, nor the total living biomass of the system once it equilibrates. As it equilibrates, its rate of change becomes zero.

Schmitt et al. published the δ^{13}C signature of the atmosphere for the past 24,000 years [26]. Their work produced a high-resolution δ^{13}C history for the atmosphere which showed that the δ^{13}C signature remained relatively constant for much of the 24,000 year record [26]. Eggleston

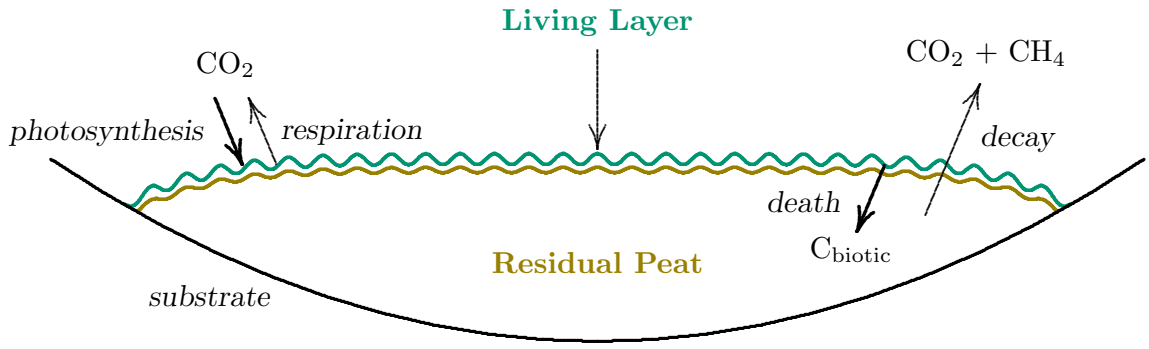

Figure 1: **Carbon circulation in a peatland.** Carbon is captured from the atmosphere in a thin living layer of photosynthetic tissue of sphagnum hummocks and hollows (green). Some of the captured carbon is respired back to the atmosphere and the rest is incorporated into the peatland, resulting from death at the lower fringe of the living layer (brown). Some carbon is released from the entire peat layer as carbon dioxide and methane at rates as indicated in [8] among others. The remainder accumulates over millennia, until disturbed by glacial or other forces.

et al. provide the $\delta^{13}C$ signature of the atmosphere for the past 120,000 years [9, 10] with slight adjustments to the past 24,000 years originally published by Schmitt et al. [26].

Over much of the past 24,000 years, the range of atmospheric $\delta^{13}C$ is from $-6.5‰$ to $-6.3‰$, but dropped sharply to $-6.7‰$ in a particular 'W' shape beginning around 17,000 years ago and ending 9,000 years ago. (Figure 4A, dotted blue curve). This drop corresponds to a period when the amount of carbon in the atmosphere was increasing substantially—from about 190 to 260 ppmv (Figure 4A, black dots/red curve). Thus the isotopic signature of the carbon entering the atmosphere during this period was not in dynamic equilibrium with the carbon already in the atmosphere, pointing to new net biological or physical sinks or sources, possibly related to glacial retreat. A better understanding of the substantial increase in carbon from 17,000 years ago may come from examining the carbon isotope signature of flows in and out of the atmosphere, leading to a better understanding of the carbon budget during the Holocene and today.

The increase in total carbon in the atmosphere since the last glacial maximum is often attributed largely to deep ocean upwelling (see discussion in [26]). Schmitt et al. consider how much upwelling, which is constrained to the falling edges of the 'W' parts of their data, can be explained by the $\delta^{13}C$ data. They determine that upwelling occurred from 17,000 to 15,000 years ago and from 13,000 to 11,500 years ago [26]. In Figure 4A, we present revised data from Eggelston et al. which shows apparent upwelling from 18,000 to 16,000 years ago and from 14,000 to 12,500 years ago [9, 10].

Schmitt et al. point out that the rising edges of the 'W' could be due to the growth of the terrestrial biosphere after the glaciers retreated, with plant growth favoring carbon-12 and thereby leaving a relative surplus of carbon-13 in the atmosphere, hence correspondingly higher δ^{13}C measurements.

In this paper we describe a method to examine the predominant behavior of abiotic and biotic pools of carbon during the Holocene. The mathematical background, algorithm, and associated computer code are detailed in the Supplementary Material. We applied this algorithm to analyze the rate at which each carbon isotope was changing in the atmosphere and determine the simplest explanation for that change. We also incorporated data on the carbon sequestration of North American peatlands in an effort to understand how the carbon budget was affected by the regrowth of part of the North American terrestrial biosphere after glacial retreat. We present the results of two representative test cases in the body of the text below. The other test cases are presented in Appendix A.

2 Methods

The algorithm examines whether changes in the atmosphere between two successive times appears to be predominantly biotic or abiotic, or a mixture of the two (Figure 2). Biotic contributions are those that are relatively light in carbon-13 and abiotic are those that are relatively heavy. If the carbon δ^{13}C ratio of carbon entering or leaving the atmosphere in a time period is contained completely within either the biotic range or the abiotic range, the algorithm attributes that change to be completely biotic or abiotic, respectively. If it falls outside the biotic and abiotic ranges or between the ranges, the change in carbon is taken to be a mixture of biotic and abiotic, with the mixture chosen to minimize the total flow of carbon in or out of the atmosphere. (Details in Supplementary Material.)

Schmitt et al. [26] proposed the regrowth of the terrestrial biosphere as a predominant mechanism driving the change in atmospheric carbon isotopes from 11,500 years ago to 6,500 years ago. Because northern peatlands are a considerable part of the terrestrial biosphere and information is available on their growth following glacial retreat ([13–15]), we used data for carbon sequestration in North American peatlands as a starting point. Carbon sequestered in other pools such as lake sediments and northern forests can be handled similarly.

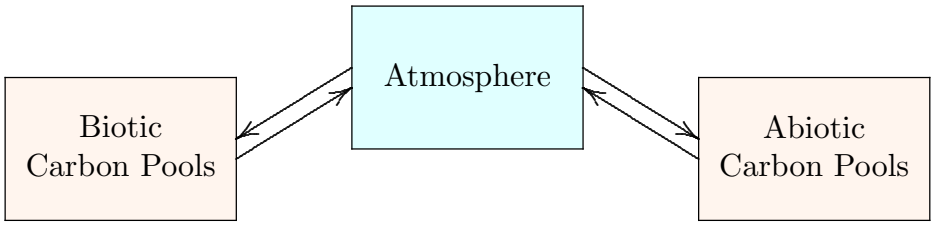

Figure 2: **Visual schematic of the algorithm.** The algorithm in the Supplementary Material determines the minimum amounts of biotic and abiotic carbon needed to explain observed changes of atmospheric carbon. For each time interval, the biotic and abiotic pools can emit carbon to or sequester carbon from the atmosphere. See the Supplementary Material for the details of the algorithm.

Schmitt et al.'s data appear in the form of total carbon dioxide (units of ppmv, parts per million by volume) and δ^{13}C content (units of permil), which we converted to total mass of carbon-12 and of carbon-13 in the atmosphere, scaling by 2.212 Pg C/ppmv [5]. Yearly time series for total carbon and δ^{13}C were then obtained by fitting a cubic smoothing spline [22] to the results and evaluating individual points along the spline.

We ran the algorithm on nine different parameter sets over the time series to examine various possibilities for flow in and out of biotic and abiotic carbon pools, using various combinations of parameters defining those pools. We then did the same thing after accounting for carbon associated with the regrowth of North American peatlands during the time [15] (Figure 3), using a characteristic δ^{13}C content for peatlands, to determine how much carbon remained unaccounted for from other components of the biosphere.

That resulted in eighteen different numerical test cases which are presented in Figures 5 and 6 (see Appendix A). The test cases explored the dependence of the results on the ranges of the δ^{13}C signatures for our abiotic and biotic pools. Since our results were qualitatively robust to realistic ranges, we present two representative results in the following section.

3 Results

A representative result from the nine test cases that do not take northern peatlands into account appears in Figure 4B and a representative of the nine cases which account for peatlands appears in Figure 4C. The horizontal axis is time relative to present and the vertical axis is the estimated

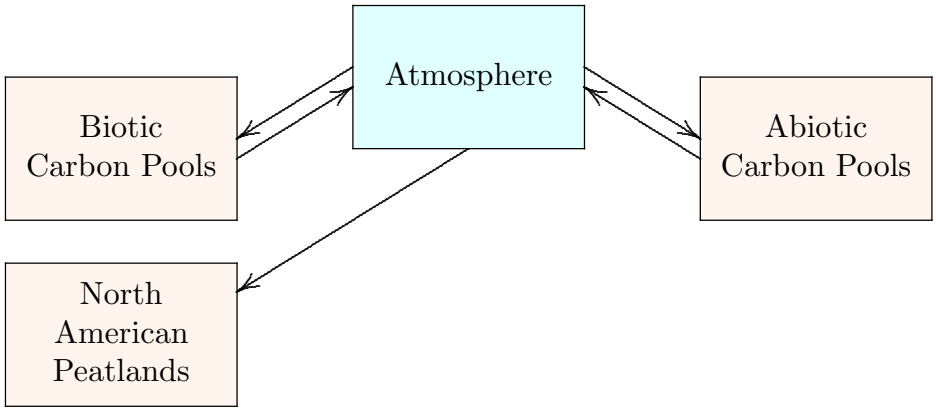

Figure 3: **Visual schematic of algorithm which incorporates peatland growth.** Same as Figure 2 except that the net sequestration of carbon into North American peatlands is explicitly accounted for. For this case, the algorithm computes the minimum amounts of biotic and abiotic carbon needed to explain both changes in the atmosphere and carbon sequestered in the peatlands. For the details of the algorithm, see the Supplementary Material.

contribution to the atmosphere from abiotic pools (orange) and biotic pools (green). Positive on the vertical axis represents a source—a flow from a carbon pool into the atmosphere, and negative on the vertical axis represents a sink, a flow from the atmosphere to a carbon pool.

Figures 4B and 4C represent test case 1-2 (see Appendix A for description of test case numbering), covering the δ^{13}C range of both C3 and C4 photosynthesis. In Figure 4B, biotic transfers of carbon (green) are minor compared with abiotic transfers. There is a signature of a biotic sink from about 10,000 years ago to about 7,000 years ago, where the biotic curve (green) falls negative, in agreement with Schmitt et al.'s analysis of their work [26].

Adding in all biotic sinks should cancel the negative biotic signature, rendering the biotic curve (green) approximately level across its range. One such biotic sink is North American peatlands. Gorham et al [15] found that those peatlands started storing carbon at a small rate beginning about 15,000 years ago and increased on a sigmoidal path to nearly 20 PgC/kyr by about 4000 years ago, then declined slightly in rate since. That alone resulted in a biotic sink of over 150 PgC since deglaciation.

High resolution δ^{13}C data over time are not available for peatlands as a whole, though studies of individual peatlands have been conducted [3, 4, 7, 19, 27, 30, 31]. Peatland δ^{13}C values range from $-32‰$ to $-16‰$, with variations predominantly attributed to seasonal weather patterns or

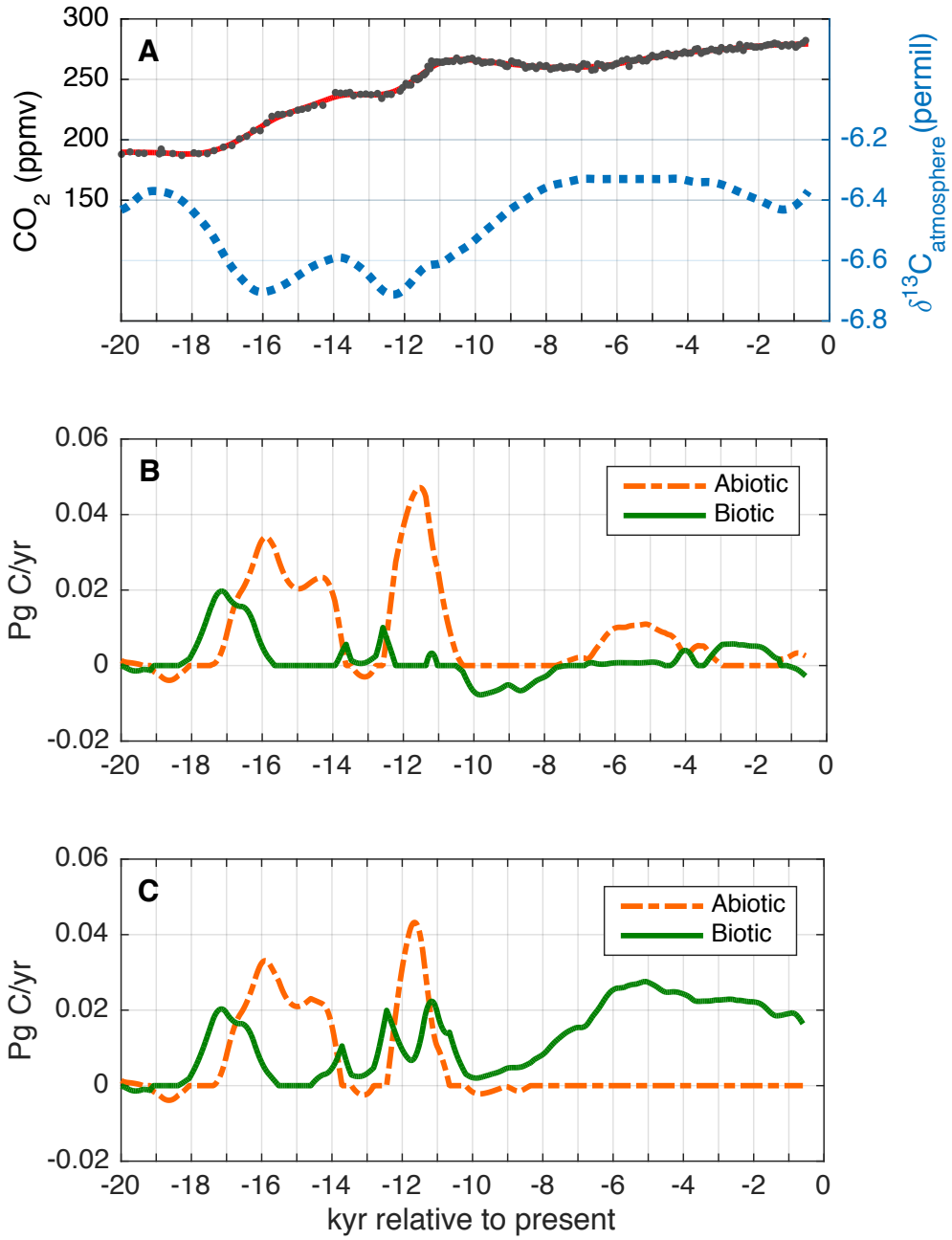

Figure 4: **Results of this study.** A: Observered atmospheric CO_2 concentrations (black dots, [20, 21]), cubic spline (solid red curve, this study), and $\delta^{13}C$ ratios (dashed blue line, [9, 10]) for the past twenty thousand years. B: The yearly contributions from the biotic (solid green line) and abiotic (dot-dash orange line) pools after analyzing only atmospheric carbon data with a biotic range of $-33‰$ to $-11‰$ and an abiotic range of $-6‰$ to $6‰$. Positive values indicate emission from the pool to the atmosphere and negative values indicate sequestration from the atmosphere into the pool. C: The yearly contributions from the biotic (solid green line) and abiotic (dot-dash orange line) pools after analyzing atmospheric carbon data and peatland sequestration data with biotic and abiotic ranges the same as the middle figure.

predominant plant type of the peatland [3, 4, 7, 19, 27, 30, 31]. Therefore we assume the average value of the available data for the δ^{13}C content of the net carbon sequestered in peatlands, which is $-25‰$. That value, coupled with the time-varying rate of peatland sequestration, gives total carbon-12 and carbon-13 in peatlands during each time interval, following the methods in the Supplementary Material. Note that to account for the peatland growth in the atmospheric data, the totals for carbon-12 and carbon-13 must be added to the atmosphere, not subtracted, as may be initially thought. Carbon in the peatland sink was in the atmosphere before it was sequestered, so the change must be accounted for in the atmosphere as well in the peatlands.

The results incorporating North American peatlands appear in Figure 4C. After accounting for peatland growth, a net biotic source is indicated starting about 11,000 years ago.

4 Discussion

Any collection of sinks or sources can be analyzed if their isotopic contents and net rates of emission or sequestration are known. Following the methods described here and in the Supplementary Materials, one needs only to compute the amounts of carbon-12 and carbon-13 emitted by the source or sequestered in the sink, then subtract or add these values to the amounts of carbon-12 and carbon-13 of the atmosphere. Through the process of incorporating sources and sinks in this way, the predominant processes affecting the Earth's carbon budget can be evaluated. When all significant sources and sinks have been accounted for, the net contributions from the biotic and abiotic pools will be zero.

There are caveats to this type of analysis. Limitations in the available data and the algorithm mean that, in some cases, ambiguities can arise where particular differing combinations of carbon ratios and flows can lead to similar conclusions. However, under physically and biologically reasonable choices of parameter values, situations which minimize flow between the pools and the atmosphere also preserve the direction of the flow, i.e. sources remain sources and sinks remains sinks.

With that in mind, partitioning the raw data for carbon content of the atmosphere during the Holocene into components that could have come from unknown biotic and abiotic sources and sinks indicates a carbon-12 deficiency in the atmosphere starting about 11,000 years ago. That suggests

a net biotic sink during deglaciation, hypothesized to be related to the regrowth of the northern biosphere as the earth warmed and large areas formerly under ice were uncovered [26].

Remarkably, however, incorporating one known biotic sink—the regrowth of North American peatlands—more than accounts for this deficiency. Apparently, from about 11,000 years ago to present, on balance carbon was flowing out of some unspecified biotic pools instead of into them.

What could those biotic pools be? That is for future discovery, perhaps through fieldwork to acquire new or more refined data on isotopic signatures of the various carbon pools, in part following the ideas presented here, to incorporate other sources and sinks into the analysis, or incorporating more subtle analyses, such as changes in atmospheric carbon-14 or oxygen concentrations. Potential candidates for further study may include coastal flooding due to deglaciation [1, 2], the desertification of the Sahara [25], carbon uptake by coral reefs [29], or anthropogenic emissions [24], among others.

Finally, it would be interesting to adapt the approach that is central to this analysis to more complex model situations. Allowing carbon pools to assume a range of values instead of the usual *a priori* fixed value could shed light on more subtle mechanisms affecting the carbon budget.

5 Conclusion

The main conclusions of this paper are as follows:

1. We present a method for analysis of atmospheric carbon data that can be extended to carbon sources and sinks as data become available. The results are robust to physically reasonable choices of parameter values.

2. Analysis of atmospheric carbon data using this method confirm earlier results concerning the data set [26].

3. Further analysis of North American peatland growth and atmospheric carbon data over the Holocene indicate a possible large source of biotic carbon starting 11,000 years ago. This could be verified through independent means or by incorporating more data into the analyses presented in this paper.

Acknowledgements

The authors would like to thank Professor Raymond Pierrehumbert for pointing out the ideas that lead to this line of inquiry. The authors acknowledge the support of the Mathematics and Climate Research Network (NSF Grants DMS-0940366 and DMS-0940363) and the Institute on the Environment at the University of Minnesota. AN was supported by an interdisciplinary graduate fellowship from the Graduate School at the University of Minnesota.

Contributions

AN made all computations and wrote the first draft of the paper. CL refactored the program which implements the data analysis to the form that appears in the Supplementary Materials. AN and RM contributed to the development of the mathematical method to account for known and unknown sources and sinks of carbon. EG motivated the development of the method, initiated the incorporation of peatlands into the analysis, and created Figure 1. All authors contributed to the editing of the manuscript. CL and RM acquired funds for the project.

Declarations of Interest

None.

References

[1] J. Abrams, et al. "Sundaland Peat Carbon Dynamics and Its Contribution to the Holocene Atmospheric CO2 Concentration," *Global Biogeochemical Cycles,* **32**: 2018. pp 704–719

[2] P. Aharon, "Meltwater flooding events in the Gulf of Mexico revisited: Implications for rapid climate changes during the last deglaciation," *Paleoceanography,* **18** (4): 2003. pp **3**-1–**3**-14

[3] R. Andersson, et al. "Elemental and isotopic carbon and nitrogen records of organic matter accumulation in a Holocene permafrost peat sequence in the East European Russian Arctic," *J. of Quat. Sci.* **27** (6): 2012. pp 545–552

[4] A. Aucour, et al. "Sources and accumulation rates of organic carbon in an equatorial peat bog (Burundi, East Africa) during the Holocene: carbon isotope constraints," *Paleo.* **150**: 1999. pp 179–189

[5] M. Battle, M. L. Bender, P. P. Tans, J. W. C. White, J. T. Ellis, T. Conway, and R. J. Francey. "Global Carbon Sinks and Their Variability Inferred from Atmospheric O2 and δ^{13}C. *Science,* **287**: 2000. pp 2467–2470.

[6] P. Ciais, P. P. Tans, J. W. C. White, M. Trolier, R. J. Francey, J. Berry, D. R. Randall, P. J. Sellers, J. G. Collatz, and D. S. Schimel. "Partitioning of ocean and land uptake of CO2 as inferred by δ^{13}C measurements from the NOAA Climate Monitoring and Diagnostics Laboratory Global Air Sampling Network." *Journal of Geophysical Research,* **100**: 1995. pp 5051–5070.

[7] G. Cristea, et al. "Carbon isotope composition as an indicator or climatic changes during the middle and late Holocene in a peat bog from the Maramures Mountains (Romania)," *The Holocene.* **0** (0): 2013. pp 1–9

[8] N. B. Dise, et al. "Carbon Emissions from Peatlands," Kolka, R. (Ed.), Sebestyen, S. (Ed.), Verry, E. (Ed.), Brooks, K. (Ed.). *Peatland Biogeochemistry and Watershed Hydrology at the Marcell Experimental Forest.* Boca Raton: CRC Press. 2011. pp 297–347

[9] S. Eggleston, et al. "Evolution of the stable carbon isotope composition of atmospheric CO2 over the last glacial cycle," *Paleoceanography,* **31**: 2016. pp 434–452

[10] [dataset] S. Eggleston, et al. "CO2 concentration and stable isotope ratios of three Antarctic ice cores covering the period from 149.4 - 1.5 kyr before 1950," *PANGAEA*: 2016. https://doi.org/10.1594/PANGAEA.859181

[11] G. D. Farquhar, J. R. Ehleringer, and K. T. Hubick. "Carbon isotope discrimination and photosynthesis," *Annu. Rev. Plant Physiol. Plant Mol. Biol.* **401** (1): 1989. pp 503–537.

[12] R. Francey, P. Tans, C. Allison, I. Enting, J. W. C. White, M. Trolier. "Changes in oceanic terrestrial carbon uptake since 1982." *Nature,* **373**: 1995. pp 326–330.

[13] E. Gorham, "Northern Peatlands: Role in the Carbon Cycle and Probable Responses to Climatic Warming." *Ecological Applications.* **1**: 1991. pp 182–195

[14] E. Gorham, et al, "Temporal and spatial aspects of peatland initiation following deglaciation in North America." *Quaternary Science Reviews.* **26**: 2007 pp 300–311

[15] E. Gorham et al, "Long-term carbon sequestration in North American peatlands." *Quaternary Science Reviews.* **58**: 2012. pp 77–82

[16] L. Husson et al, "Reef Carbonate Productivity During Quaternary Sea LevelOscillations," *Geochemistry, Geophysics, Geosystems.* **19**: 2018 pp 1148–1164

[17] P. Köhler et al. "Quantitative interpretation of atmospheric carbon records over the last glacial termination," *Global Biogeochem. Cycles* **19** (4): 2005. GB4020

[18] P. Kortelainen, et al. "A large carbon pool and small sink in boreal Holocene lake sediments," *Gobal Change Biology* **10**: 2004. pp 1648–1653

[19] J. Krüger, et al. "Degradation changes stable carbon isotope depth profiles in pala peatlands," *Biogeosciences.* **11**: 2014. pp 3369–3380

[20] [dataset] D. Luthi, et al, "High-resolution carbon dioxide concentration record 650,000-800,000 years before present." *Nature*, **453**: 2008. pp 379–382, doi:10.1038/nature06949, URL: ftp://ftp.ncdc.noaa.gov/pub/data/paleo/icecore/antarctica/epica_domec/edc-co2-2008.txt

[21] E. Monnin et al. "Atmospheric CO2 Concentrations over the Last Glacial Termination," *Science* **291**: 2001. pp 112–114

[22] C. Reinsch. "Smoothing by Spline Functions." *Numerische Mathematik,* **10**: 1967. pp 177–183

[23] J. Roundick and M. Winderbourn. "Carbon Isotopes and Carbon Flow in Ecosystems." *BioScience,* **36** (3): 1986. pp 171–177

[24] W. Ruddiman. "The Anthropocene," *Annu. Rev. Earth Palnet. Sci.* **41**: 2013. pp 45–68

[25] M. Scheffer, et al, "Catastrophic shifts in ecosystems," *Nature,* **413**: 2001. pp 591–596

[26] J. Schmitt, et al. "Carbon Isotope Constraints on the Deglacial CO2 Rise from Ice Cores," *Science.* **336**: 2012. pp 711–714

[27] G. Skrzypek, et al. "The carbon stable isotopic composition of mosses: A record of temperature variation," *Organic Geochemistry.* **38**: 2007. pp 1770–1781

[28] D. M. Sigman et al. "The polar ocean and glacial cycles in atmospheric CO2 concentration," *Nature* **466**: 2010. pp 47–55

[29] A. Vecsei and W. Berger, "Increase of atmospheric CO2 during deglaciation: Constraints on the coral reef hypothesis from patterns of deposition," *Global Biogeochemical Cycles,* **18**: 2004. **GB1035** 1–7

[30] J. Zhang, et al. "Holocene monsoon climate documented by oxygen and carbon isotopes from lake sediments and peat bogs in China: a review and synthesis," *Quat. Sci. Rev.* **30**: 2011. pp 1973–1987

[31] W. Zhong, et al. "Carbon isotope evidence of last glacial climate variations in the tropical NW Leizhou Peninsula, South China," *Boreas.* **41**: 2012. pp 102–112

A Supplementary Figures

Below are the results of eighteen different numerical test cases for different ranges for abiotic (orange, dot-dashed) and biotic (green, solid) δ^{13}C signatures. We organize these test cases by a pair of numbers, i–j, with i representing biotic values and j representing abiotic values. Test cases with $i = 1$ (top row) have a biotic carbon δ^{13}C of the full range of $-33‰$ to $-11‰$, representing much of the full range of signatures present in biological material [11, 23]. Test cases with $i = 2$ (middle row) have a biotic carbon δ^{13}C ranging from $-16‰$ to $-11‰$, the typical range for C4 photosynthesis [11, 23], and those with i = 3 (bottom row) have a biotic carbon δ^{13}C ranging from $-33‰$ to $-24‰$, the typical range for C3 photosynthesis [11, 23].

Since the dissolved carbon in the surface and deep ocean have isotopic signatures close to the standard (0‰) [6, 12, 17, 28], test cases for the abiotic pools define ranges close to the standard. Test cases with $j = 1$ (left column) have an abiotic carbon δ^{13}C range of $-10‰$ to $0‰$. Test cases with $j = 2$ (middle column) have an abiotic carbon δ^{13}C range of $-6‰$ to $6‰$, and those with $j = 3$ (right column) have an abiotic carbon δ^{13}C range of $0‰$ to $10‰$.

Figure 5 shows all i–j combinations only considering atmospheric carbon data [9, 10]. In all runs, the biotic pools (green, solid) have two major peaks of emissions around 17,000 and 13,000 years ago and sequester carbon from around 12,000 years ago to about 7,000 years ago. The abiotic pools (orange, dot-dashed) emit carbon for most of the time series in all runs, sequestering carbon for short time periods around 19,000 and 13,000 years ago. Runs with a higher range for the abiotic pools ($j = 2$ and $j = 3$) have greater contributions from the biotic pools relative to the lower ranges ($j = 1$), both when the biotic pool is emitting and sequestering carbon. All cases are qualitatively similar to Case 1-2 which is presented as a representative of this analysis in Figure 4B.

Figure 6 shows all i–j combinations considering both atmospheric carbon data [9, 10] and peatland growth [15]. After accounting for the growth of peatlands, all cases show a source of biotic carbon starting about 12,000 to 10,000 years ago. This new biotic source is accompanied with either a decrease in the abiotic source during this time period (to either no flow in $i = 1$ or a sink $i = 2$) or no change in the abiotic source, suggesting that during the period that the peatlands were growing, there was a source of biotic carbon with similar, if not greater, magnitude to the peatlands. All cases are qualitatively similar to Case 1-2 which is presented as a representative of

this analysis in Figure 4C.

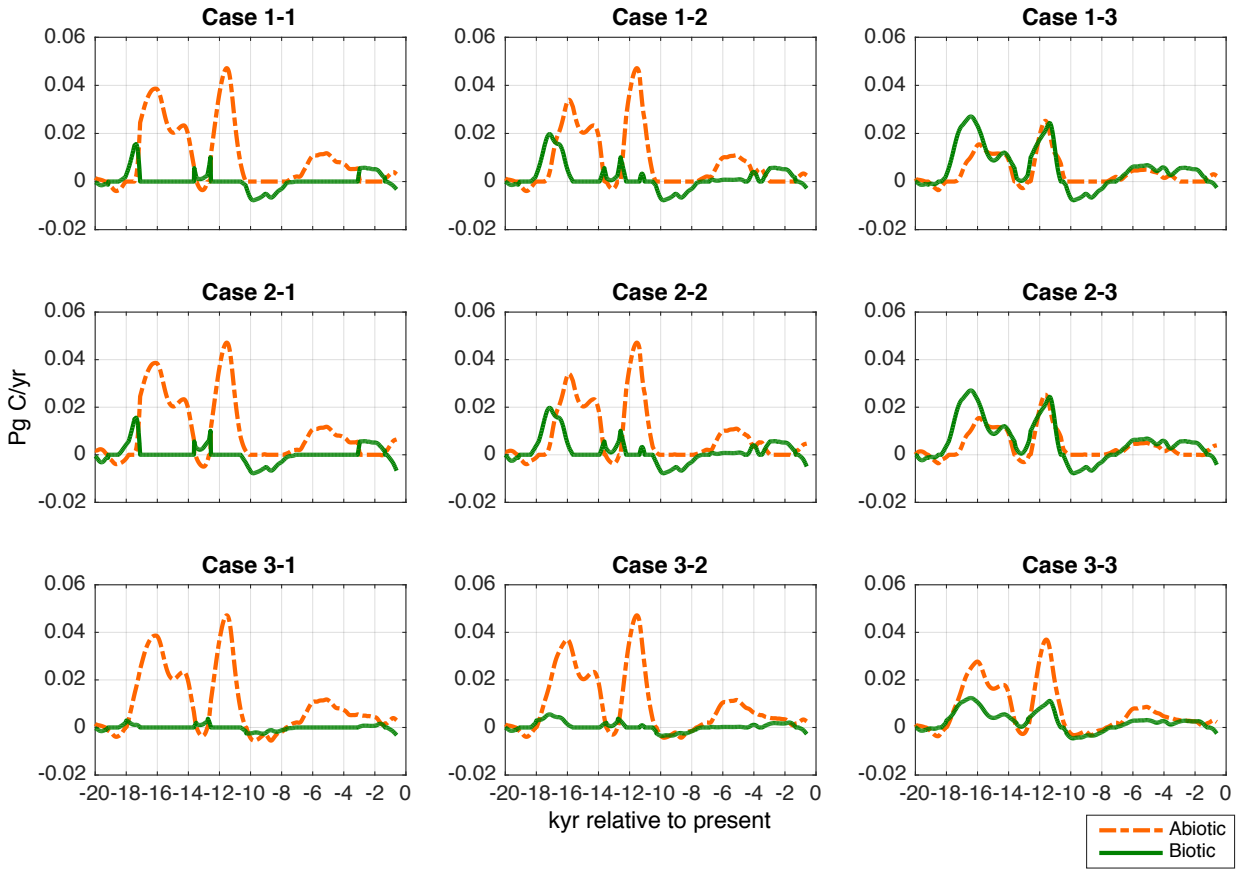

Figure 5: **Test cases of this study.** The yearly contributions from the biotic (solid green line) and abiotic (dot-dash orange line) pools after analyzing the Eggleston et al (2016) atmospheric carbon data [9,10] for nine different parameter combinations. See text for description of numerical labelling for the different cases. Figure 4B is Case 1-2. Positive values indicate a source and negative values indicate a sink of carbon.

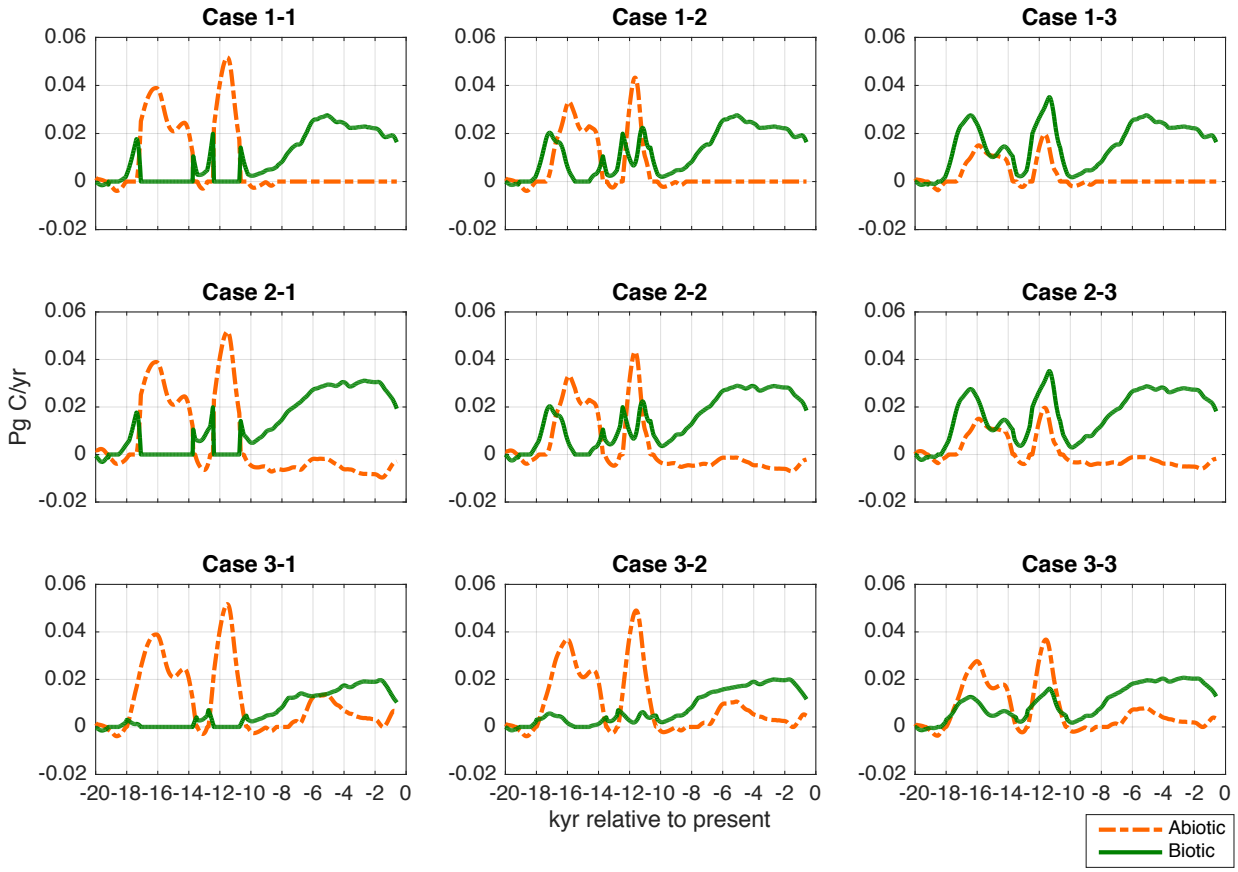

Figure 6: **Test cases which incorporate peatland growth.** The yearly contributions from the biotic (solid green line) and abiotic (dot-dash orange line) pools after analyzing the Eggleston et al (2016) atmospheric carbon data [9, 10] and peatland growth [15] for nine different parameter combinations. See text for description of numerical labelling for the different cases. Figure 4C is Case 1-2. Positive values indicate a source and negative values indicate a sink of carbon.

APPENDIX: COMPUTER CODE

This appendix carries the computer code to analyse carbon dioxide in the atmosphere and flows in and out of abiotic and biotic carbon pools. It includes background material that may be needed by those working on the code to understand it. It is presented in a form of pseudo-code that is readily translated to specific languages.

1. Carbon isotopes

Carbon has three natural isotopes—carbon 12, 13, and 14. The abundance of carbon 12 is about 99% of total carbon, carbon 13 is about 1%, and carbon 14 is negligible. The first two are stable but carbon 14 has a half-life of about 5700 years.

All three forms of carbon are used by living things, but the lighter carbon 12 is taken up in greater proportions during photosynthesis, and the proportion tends to be retained in herbivores and carnivores nearby in the food web. Plants with a C4 photosynthetic pathway incorporate less carbon 12 than those with a C3 pathway. Differences in proportions are slight, however, as follows.

Category	^{13}C/C
Marine foraminifera (standard)	1.111%
Volcanic plume (Chiodini et al 2010)	1.110%
Plants with C4 photosynthetic pathway	1.098%
Plants with C3 photosynthetic pathway	1.082%

These small differences are intentionally magnified by measuring the ratio of carbon 13 to carbon 12, relative to a standard, then normalized to 0, and finally expressed in mils. This is called delta-carbon-13, δ^{13}C.

$$\delta^{13}\mathrm{C} = \left(\frac{\left.\frac{^{13}\mathrm{C}}{^{12}\mathrm{C}}\right|_{\text{sample}}}{\left.\frac{^{13}\mathrm{C}}{^{12}\mathrm{C}}\right|_{\text{standard}}} - 1 \right) \times 1000 \tag{A1}$$

The standard is a cretaceous marine fossil with a ^{13}C/ ^{12}C ratio of 0.0112372. That, with the percentages above, leads to the following δ^{13}C values.

$$\begin{aligned}
\delta^{13}\mathrm{C}\big|_{\text{standard}} &= \big(0.01111/(1-0.01111)/0.0112372 - 1\big) \times 1000 = \quad 0 \\
\delta^{13}\mathrm{C}\big|_{\text{volcano}} &= \big(0.01110/(1-0.01110)/0.0112372 - 1\big) \times 1000 = -1 \\
\delta^{13}\mathrm{C}\big|_{\text{C4}} &= \big(0.01098/(1-0.01098)/0.0112372 - 1\big) \times 1000 = -12 \\
\delta^{13}\mathrm{C}\big|_{\text{C3}} &= \big(0.01082/(1-0.01082)/0.0112372 - 1\big) \times 1000 = -27
\end{aligned}$$

APPENDIX: COMPUTER CODE

2. Carbon pools

Carbon 12 and 13 concentrations in the atmosphere are averaged monthly at various weather stations around the globe, and are also available in the fossil record. Total carbon in the atmosphere fluctuates, but the ratio of carbon 13 to 12 also fluctuates. Biotic pools contain relatively less carbon 13 than abiotic pools, and that provides a way to estimate flows in and out.

Figure A1 represents the two main carbon pools and the atmosphere. Many sub-pools are involved—terrestrial, oceanic, glacial, and subterranean. Peatlands take part, lake sediments, prairie soils, forest biomass, volcanic plumes, rocks, and more—each with a distinct combination of carbon 12 and 13. The ^{13}C/C ratio flowing to or from the abiotic pool at time t is $\alpha(t)$ and the corresponding ratio in the biotic pool at time t is $\beta(t)$. These ratios vary as different sub-pools absorb or release carbon.

FIGURE A1

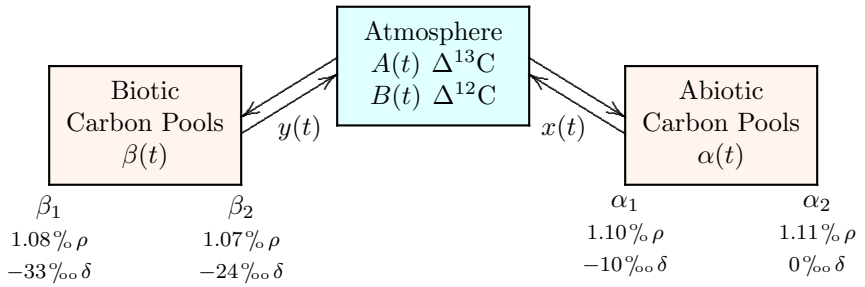

The lowest and highest values for the ^{13}C/C ratios representing the set of abiotic pools are α_1 and α_2, respectively, and the corresponding values for the set of biotic pools are β_1 and β_2. These are not functions of time, but they may be varied from run to run to test hypotheses about the pools. Shown below these parameters in Figure A1 are representative values for the ratios as percentages (ρ) and as corresponding δ^{13}C values in mils (δ) but the α_i and β_i are processed in the program simply as ratios, not as percentages or δ^{13}C mils.

The increment or decrement of carbon 13 in the atmosphere between times t and $t + \Delta t$ is $A(t)$ and the corresponding value for carbon 12 is $B(t)$. These are related to the empirical values reported by the climate stations around the globe, or in the fossil record, and here both are measured in petagrams per time unit.

Finally in Figure A1, $x(t)$ and $y(t)$ represent the total carbon contributed by the set of abiotic and biotic pools, respectively, at time t, measured in petagrams.

3. Preprocessing input data

The data available are total carbon dioxide in the atmosphere, measured in parts per million by volume, and the δ^{13}C ratio of the atmosphere, measured in mils as in Equation A1. Parts per million by volume can be converted to mass by taking 2.212 petagrams of carbon in the atmosphere for each part per million. Then the δ^{13}C ratio can partition that mass into carbon 12 and carbon 13.

For a given δ^{13}C ratio, the portion of the total carbon that is carbon 13 is obtained by starting with Equation A1,

$$q = \left.\frac{^{13}\mathrm{C}}{^{12}\mathrm{C}}\right|_{\text{sample}} = \left(\frac{\delta^{13}\mathrm{C}}{1000} + 1\right) \left.\frac{^{13}\mathrm{C}}{^{12}\mathrm{C}}\right|_{\text{standard}} \tag{A2}$$

Now computing

$$\frac{1}{1+q} = \frac{1}{1 + {}^{13}\mathrm{C}/{}^{12}\mathrm{C}} = \frac{^{12}\mathrm{C}}{^{12}\mathrm{C} + {}^{13}\mathrm{C}} \tag{A3}$$

gives the proportion of total carbon that is carbon 12. The complement of that is the proportion that is carbon 13.

$$1 - \frac{1}{1+q} = \frac{^{13}\mathrm{C}}{^{12}\mathrm{C} + ^{13}\mathrm{C}} \tag{A4}$$

Thus values for A and B can be computed from total carbon in the atmosphere and its δ^{13}C.

4. Flow among atmosphere and carbon pools

The main goal is to identify any long-term trends in the biotic and abiotic pools, using the empirical data for carbon flowing in and out of the atmosphere as a guide. For any time period,

$$A(t) = \alpha(t)\, x(t) + \beta(t)\, y(t)$$

and simultaneously

$$A(t) + B(t) = x(t) + y(t)$$

As long as α and β differ, the solution of those two linear equations gives the flows in and out of the pools.

$$\begin{aligned} x(\alpha, \beta) &= \frac{A - (A+B)\beta}{\alpha - \beta} \\ y(\alpha, \beta) &= \frac{A - (A+B)\alpha}{\beta - \alpha} \end{aligned} \tag{A5}$$

The flows are identical in form except for the interchange of α and β.

Choosing the α and β ratios participating each time step, among all the possible values for all the various unknown sub-pools, is the next step. An occam's-razor approach to choosing them, in absence of other information, is to keep the total amount of carbon exchanged in a time step to a minimum. Definitive values are provided by the following considerations.

If the carbon ratio in the atmospheric flow corresponds to a possible ratio of one of the two carbon pools—biotic or abiotic—then the total flow is minimized by attributing all of the atmospheric exchange to that pool and none to the other pool. If it is between the the two sets of pools, then contributions from both pools must be involved. It can be shown that attributing flow at the highest concentration from the biotic pool and the lowest concentration from the abiotic pool minimizes the total flow. Finally, if the atmospheric ratio is either above or below both pools, it can be likewise shown that attributing flow at the lowest concentration from the biotic pool from the abiotic pool minimizes the total flow. These consideration are reflected in the code below.

5. Pseudocode

To allow complete evaluation of the algorithm, and to support modifications, we present the algorithm in a form of pseudo-code inspired by and simplified from the programming languages C, R, and Python. In addition, code lines begin with a vertical bar (|), as do comments on the right, in what we call "document format."

The pseudo-code is two-dimensional, as in the language Python, so that indentation completely defines the nested structure without use of bracketing characters such as '{' and '}'. Statement separators such as semicolon ('**;**') are likewise unused. Variables and function names are italicized and flow control and reserved words are bolded.

Computations follow a left-to-right, top-to-bottom flow. Thus the assignment operator is represented as '$\rightarrow$', similar to possibilities in R, and also as represented in von Neumann's early computer programs. A

compound assignment such as '$x \to y \to z$' first transfers x to y, then transfers y to z. Upon completion all three thus carry the same value. Flow control with if–then–else and looping are similar to other languages.

Mathematical symbols may appear directly in the pseudocode for clarity, rather than being spelled out. For example, 'α_1' may be used rather than 'alpha1'. Case matters, so that a is different than A. Simple functions are defined by the form '$H(\text{parameters}) \equiv \text{expression}$'. For example, one can write '$\mu(x, y) \equiv (x + y)/2$'. Variables not defined start out at 0. Operator precedence is that of C.

Equivalent versions of this algorithm translated into operational C or FORTRAN are available from the authors upon request.

6. Algorithm

The program begins with the definition of three functions and initialization of bounds of the carbon pools.

On entry to the program, input consists of a data file in order of increasing time. The input data have three columns.

- n Sequence number representing a variable-length time step, for reference.
- A Flow of carbon 12 during the time step, in petagrams. Positive is flow from carbon pools to the atmosphere, negative is the reverse.
- B Flow of carbon 13 during the time step, in petagrams. Positive is flow from carbon pools to the atmosphere, negative is the reverse.

On exit from the program, output consists of a data file in order of increasing time. The output data have seven columns.

- n A sequence number representing the time step, matching the first column in the input file.
- A Flow of carbon 12 during the time step, matching the corresponding column in the input file.
- B Flow of carbon 13 during the time step, matching the corresponding column in the input file.
- x Total carbon entering or leaving the set of abiotic carbon pools during the time step, in petagrams.
- y Total carbon entering or leaving the set of biotic carbon pools during the time step, in petagrams.
- α Ratio of carbon 13 to total carbon in the flow represented by x in this time step.
- β Ratio of carbon 12 to total carbon in the flow represented by y in this time step.

$F_x(a, b, A, B) \equiv (A - (A + B) * b)/(a - b)$ $F_y(a, b, A, B) \equiv (A - (A + B) * a)/(b - a)$	Function, abiotic flow. Function, biotic flow.
$R(d) \equiv 1 - 1/(1 + (d/1000 + 1) * 0.0112372)$	Function, δ^{13}C to ^{13}C/$^{12+13}$C conversion.
$R(-33) \to \beta_1 \quad R(-24) \to \beta_2$ $R(-10) \to \alpha_1 \quad R(\quad 0) \to \alpha_2$	Low and high ratios for the biotic and abiotic pools, respectively.
repeat until *end-of-file*: $\quad$ *read*$(n, A, B) \quad A/(A+B) \to r$	Read the next time period and calculate the ratio of ^{13}C/$^{12+13}$C exchange.
$\quad$ **if** $\alpha_1 \le r \le \alpha_2$: $\quad\quad r \to \alpha \quad 0 \to \beta \to y \quad A+B \to x$	If the ratio is in the abiotic range, ascribe all carbon to the abiotic pool.
$\quad$ **else if** $\beta_1 \le r \le \beta_2$: $\quad\quad r \to \beta \quad 0 \to \alpha \to x \quad A+B \to y$	In contrast, if it is in the biotic range, ascribe all carbon to the biotic pool.
$\quad$ **else if** $\beta_2 < r < \alpha_1$: $\quad\quad \alpha_1 \to \alpha \quad \beta_2 \to \beta \quad F_x(\alpha, \beta, A, B) \to x \quad F_y(\alpha, \beta, A, B) \to y$	If the ratio is between the pools, use the heaviest biotic and lightest abiotic values.
$\quad$ **else** $\quad\quad \alpha_2 \to \alpha \quad \beta_1 \to \beta \quad F_x(\alpha, \beta, A, B) \to x \quad F_y(\alpha, \beta, A, B) \to y$	Otherwise, choose the ratio that minimizes total carbon flow among the pools.
$\quad X+x \to X \quad Y+y \to Y$ $\quad$ *write*$(n, A, B, x, y, \alpha, \beta)$	Accumulate the flows to and from both pools and record the results.

APPENDIX: COMPUTER CODE

7. Sample Output

For testing and reference, below is an excerpt of the algorithm's output for the data presented in columns `A` and `B`. The data are represented in excess precision for purposes of validation.

```
|n   |A              |B              |x         |y         |alpha    |beta
|  1 | 0.023005443570 | 2.14959455600 |-0.962217 | 3.134817 |0.011112 |0.010750
|  2 | 0.001417597648 | 0.08378240235 | 1.383085 |-1.297885 |0.011112 |0.010750
|  3 | 0.031941570710 | 2.88615842900 | 1.848496 | 1.069604 |0.011002 |0.010849
|  4 |-0.016522470420 |-1.47447753000 |-1.491000 | 0.000000 |0.011081 |0.000000
|  5 |-0.057460835100 |-5.22493916500 |-1.004417 |-4.277983 |0.011002 |0.010849
   :    :               :               :          :          :         :
|402 |-0.065321962920 |-6.00517803700 | 0.000000 |-6.070500 |0.000000 |0.010761
|403 |-0.026066237920 |-2.38083376200 | 0.000000 |-2.406900 |0.000000 |0.010830
|404 | 0.011369124930 | 1.05363087500 |-0.218214 | 1.283214 |0.011112 |0.010750
|405 | 0.037801727970 | 3.43409827200 | 0.888428 | 2.583472 |0.011002 |0.010849
|406 | 0.026061362910 | 2.38083863700 | 0.000000 | 2.406900 |0.000000 |0.010828
```